JOURNAL OF THERMOPHYSICS AND HEAT TRANSFER
Vol. 6, No. 2, April–June 1992

Natural Convection Heat Transfer in Rectangular Cavities Partially Heated from Below

M. Hasnaoui,* E. Bilgen,† and P. Vasseur†
Ecole Polytechnique de Montréal, Montréal, Quebec H3C 3A7, Canada

Natural convection in an enclosed cavity with localized heating from below has been investigated by a finite difference procedure. The upper surface is cooled at a constant temperature and a portion of the bottom surface is isothermally heated while the rest of the bottom surface and the vertical walls are adiabatic. Parameters of the problem are the cavity aspect ratio (A = 1 and 2), dimensionless length (B = 0.06 to 1.0) and position of the heat source with respect to the vertical symmetry line of the cavity (ϵ = −0.6 to 0.7), the Prandtl number and the Rayleigh number (Ra = 0 to 5 × 10^6). The effects of the thermophysical and geometrical parameters on the fluid flow and temperature fields have been studied. The existence of multiple steady-state solutions and the oscillatory behavior for a given set of the governing parameters are demonstrated.

Nomenclature

A = aspect ratio, L'/H'
B = dimensionless length of heat source, ℓ'/L'
g = acceleration due to gravity, m/s²
H' = cavity height, m
h = local heat transfer coefficient, W/m²·K
$\bar{h}$ = average heat transfer coefficient, W/m²·K
k = thermal conductivity of fluid, W/m·K
L' = cavity width, m
ℓ' = length of heat source, m
m, n = wave numbers of initial disturbance, Eq. (15)
Nu = Nusselt number based on cavity height, $\bar{h}H'/K$
Pr = Prandtl number, ν/α
p' = pressure, Pa
Q = dimensionless heat transfer averaged over all lines of the mesh grid
Ra = Rayleigh number, $(g\beta\Delta T'H'^3)/(\nu\alpha)$
S_f = dimensionless reduced shape factor
T = dimensionless temperature of fluid, $(T' - T'_C)/(T'_H - T'_C)$
T' = temperature of fluid
$\Delta T'$ = temperature difference, $(T'_H - T'_C)$
t = dimensionless time, $t'\alpha/H'^2$
t' = time, s
u, v = dimensionless velocities in x and y directions, $(u', v')\,H'/\alpha$
u', v' = velocities in x' and y' directions, m/s
x, y = dimensionless Cartesian coordinates, $(x', y')/H'$
x', y' = Cartesian coordinates, m
α = thermal diffusivity, m²/s
β = volumetric coefficient of thermal expansion, K^{-1}
ϵ = dimensionless position of heat source, $2\epsilon'/L'$
ϵ' = position of heat source, m
ν = kinematic viscosity, m²/s
ρ = fluid density, kg/m³
ω' = vorticity, s^{-1}
Ψ = dimensionless stream function, Ψ/α
Ψ_{ext} = extremum value of Ψ (either Ψ_{max} or Ψ_{min})
Ω = dimensionless vorticity, $\omega'H'^2/\alpha$

Subscripts
cr = critical value
h = heated wall
ext = extremum value
max = maximum value
min = minimum value

Superscript
′ = dimensional variables

Introduction

THE natural convection in enclosures has been of interest to engineering applications for many years. Well known examples are the thermal design of buildings, solar collectors, circulation of fluid in electronic or computer equipment, and thermal energy storage systems. These applications require knowledge of natural convection in various geometries and angle of the geometry to the gravitational field. Ostrach[1] and Catton[2] have reviewed the work done on various internal flow problems.

Most of the previous work has addressed natural convection in enclosures due either to a vertically or horizontally imposed temperature difference. However, little work has been carried out on flows driven by localized heating from below. Torrance and Rockett[3] numerically studied the convection of air in a vertical cylindrical enclosure, induced by a small hot spot centrally located on the bottom. Solutions were obtained for Rayleigh numbers from 2.84 × 10^4 to 2.84 × 10^{10}. The theoretical flows were found to be in excellent agreement with experimentally observed laminar flows ($Ra \leq 8.5 \times 10^8$), which are discussed in a companion paper by Torrance et al.[4] Experimental results were also presented for the case of rectangular geometry but were not complemented by an analytic investigation. Tamotsu et al.[5] experimentally and numerically investigated natural convection in a rectangular enclosed cavity, of which a part of the bottom was heated and the other walls were kept at a low constant temperature. The influence of the Rayleigh number, up to Ra = 6.9 × 10^5, was discussed and the results of the computation were observed to agree qualitatively with experimental observations. The natural convection in an inclined box with the half of the lower surface heated and the other half insulated was investigated experimentally and numerically by Chao et al.[6] It was found that the asymmetry due to insulating half of the heated surface resulted in circulations for all positive Rayleigh numbers. An experimental investigation was conducted by Kamotani et al.[7] to study natural convection heat transfer in a water layer with localized heating from below. The flows were driven by main-

Received Nov. 30, 1990; revision received April 24, 1991; accepted for publication April 25, 1991. Copyright © 1991 by the Americar Institute of Aeronautics and Astronautics, Inc. All rights reserved.
*Graduate Assistant.
†Professor.

taining a small circular heat source, centrally located on the bottom, at a uniform temperature. For a shallow cavity the flow within the fluid layer was found to have a single elongated unicellular pattern. As the aspect ratio was increased, the flow structure became more complex with the appearance of two secondary cells superposed on the basic unicellular flow structure, one near the center and the other near the side wall. The tendency for the flow to give rise to one eddy near the side wall as Rayleigh number increased was also observed by Torrance and Rockett[3] and Torrance et al.[4] A few studies have also been conducted on enclosure flows driven by localized heating from below in a medium with ambient stratification. This particular topic has been reviewed recently by Fuseki and Farouk.[8]

The present study considers the recirculating flows induced in a rectangular two-dimensional enclosure by localized heating from below. Recently, it was demonstrated that, under certain conditions, multiple steady-state solutions can be sustained within a porous material heated from its bottom (Walch and Dulieu,[9] Caltagirone and Bories,[10] Moya et al.,[11] Robillard et al.[12] among others). This multiplicity is not merely theoretical as there is experimental evidence for at least two different stably convective flows under identical heating and geometric conditions (Acosta et al.[13]). Here also multiple steady-state solutions are expected and the conditions of their occurrence are studied.

Problem Formulation

Consider the motion of a viscous fluid within a rectangular cavity of length L' and height H' (see Fig. 1). It is assumed that the flow and heat transfer are two-dimensional. The lower surface is maintained at a temperature T'_H, which is higher than the temperature T'_C of the top. The rest of the bottom wall is insulated. The distance between the center of the heated element and the vertical axis of symmetry of the cavity is ϵ', such that when $\epsilon' = 0$ the heat source is centrally located at the bottom surface.

All properties of the fluid are considered constant, except the density of the fluid that gives rise to the buoyancy force. This so-called Boussinesq approximation is practically valid for small temperature and pressure variations within the flow region. Neglecting viscous dissipation, the governing equations are written as

$$\frac{\partial u'}{\partial x'} + \frac{\partial v'}{\partial y'} = 0 \tag{1}$$

$$\frac{Du'}{Dt'} = -\frac{1}{\rho_0}\frac{\partial p'}{\partial x'} + \nu\nabla^2 u' \tag{2}$$

$$\frac{Dv'}{Dt'} = -\frac{1}{\rho_0}\frac{\partial p'}{\partial y'} - g[1 - \beta(T' - T'_C)] + \nu\nabla^2 v' \tag{3}$$

$$\frac{DT'}{Dt'} = \alpha\nabla^2 T' \tag{4}$$

where ρ_0 is the reference density taken at T'_C.

Using nondimensional variables defined in the nomenclature and introducing the stream function and vorticity, the dimensionless governing equations are written in stream function-vorticity formulation as

$$\frac{D\Omega}{Dt} = -RaPr\frac{\partial T}{\partial x} + Pr\nabla^2\Omega \tag{5}$$

$$\nabla^2\Psi = -\Omega \tag{6}$$

$$\frac{DT}{Dt} = \nabla^2 T \tag{7}$$

where

$$u = -\frac{\partial\Psi}{\partial y} \qquad v = \frac{\partial\Psi}{\partial x} \tag{8}$$

$$\Omega = \left(\frac{\partial u}{\partial y} - \frac{\partial v}{\partial x}\right) \tag{9}$$

No-slip boundary conditions are considered for the velocity components along the walls and the vorticity boundary condition is obtained directly from the definition, Eq. (9). For the temperature, following boundary conditions are used:

$$\begin{aligned} T &= 1 \quad \text{for heated surfaces} \\ T &= 0 \quad \text{for } y = 1 \\ \left.\frac{\partial T}{\partial n}\right|_{n=0} &= 0 \quad \text{for adiabatic surfaces} \end{aligned} \tag{10}$$

where n denotes the normal at the surface.

The governing equations and geometry of the cavity introduce five dimensionless parameters, which are the Rayleigh number Ra, the Prandtl number Pr, and the geometric parameters ϵ, A, and B. The geometric parameters ϵ and B denote the position and dimensionless length of the heated element, respectively. The case with $B = 1$ corresponds to natural convection in a cavity fully heated from below, while the case $\epsilon = 0$, $B < 1$ corresponds to a cavity with a hot spot centrally located on the bottom.

Numerical Method

Equations (5–7) with appropriate boundary conditions were solved with a time-marching, finite-difference technique. The first and second derivatives were approximated by central differences and the time derivatives by a first order forward difference. The finite difference form of the vorticity transport and energy equations was written in conservative form for the nonlinear convective terms in order to preserve the conservative property.

The numerical results presented here employed a 41 × 41 or 61 × 31 mesh in the x and y directions for the aspect ratio of 1 or 2, respectively. The grid independence of the solutions has been checked with these grid configurations. For instance, when $Ra = 5 \times 10^5$, $A = 1$, $B = 0.5$, and $\epsilon = 0$, Table 1 shows the mesh influence on the results.

The computations were done on an IBM 3090 computer. Both heat flux and circulation were monitored as sensitive indicators of the approach to steady state. Time steps as low as 0.0004 were used in obtaining stable solutions. The multiplicity of solutions was a main objective of this study. Hence, the entire domain was considered without symmetry lines.

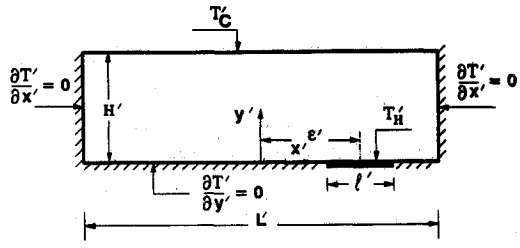

Fig. 1 Geometry and boundary conditions of the problem.

Table 1 The mesh influence on the results

Mesh	$\lvert\Psi_{ext}\rvert$	$\bar{Q}$
33 × 33	55.24	5.046
41 × 41	55.34	5.046
53 × 53	55.38	5.044

For each time step the dimensionless heat transport for a given horizontal line of the network was determined by means of the expression

$$Q = \int_{-1/2}^{1/2} \left(\frac{\partial T}{\partial y} - vT \right) dx \tag{11}$$

The overall heat transfer $\bar{Q}$ was obtained by taking the average of Q at all lines. It is also appropriate at this stage to define a mean Nusselt number, based on the height of the cavity as

$$Nu = \frac{\bar{Q}}{\bar{Q}_C} \tag{12}$$

where $\bar{Q}_C$ is the dimensionless heat transfer by pure conduction.

Hahne and Schalling[14] give the dimensionless heat transfer $\bar{Q}_C$ for pure conduction with $\epsilon = 0$ as

$$\bar{Q}_C = \frac{1}{1 + 0.5S_f} \tag{13}$$

where the dimensionless reduced shape factor is given approximately by

$$S_f = \frac{1}{\pi} \ln \frac{2}{1 - \sin 0.5\pi(1 - 2B)} \tag{14}$$

In this investigation, the multiplicity of steady states for a given geometry is explored. Naturally, the time-dependent governing Eqs. (5–7) can be presumed to have a unique solution as in an initial value problem. So when multiple steady states do exist, initial conditions determine the final steady state achieved. Thus, in addition to the boundary conditions, Eq. (10), it is also necessary to specify some initial conditions at time $t = 0$. This is done by using a "stirred" flow as the initial condition of the evolutive problem; this is written as follows:

$$\Psi = \Psi_p \sin m\pi x \sin n\pi y \tag{15}$$

where Ψ_p is the amplitude of the initial perturbation. In order to obtain antinatural solutions the initial "stirred" flow had to be made large enough in order to "survive" over the natural state. A value of $\Psi_p = 40$ has been chosen for all the antinatural solutions presented in this study. Provided that Ψ_p is large enough, the resulting antinatural solutions have been found numerically to be independent of the amplitude of the initial perturbation.

The accuracy of the numerical model was verified by comparing results from the present investigation with several results reported in the literature. Results for the limiting case of a cavity fully heated from below $B = 1$ were compared with those obtained by Ozoe et al.[15] The numerical model was also validated by comparing the results with the bench mark solution of De Vahl Davis[16] for a square cavity with vertical sides differentially heated. Maximum differences were found to be within 2% with the first case and 4% with the

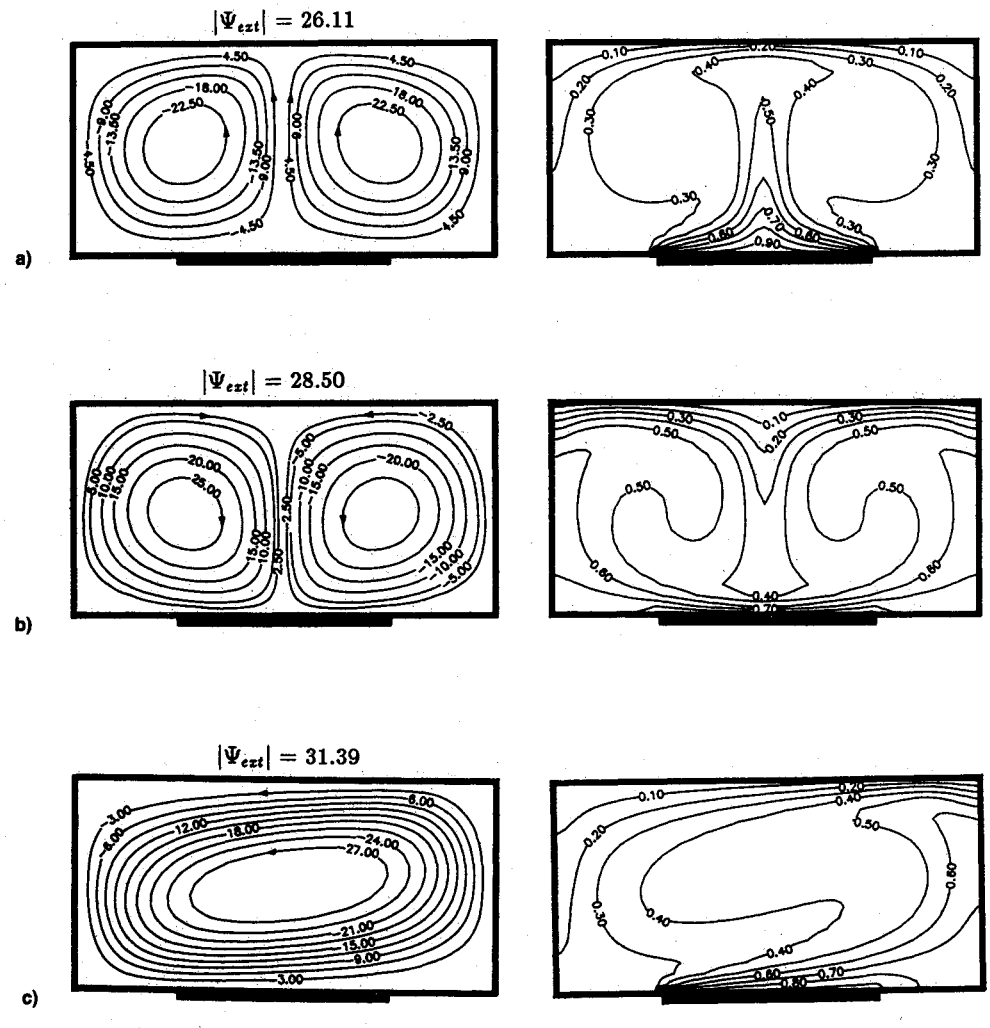

Fig. 2 Steady-state streamlines and isotherms for $Ra = 10^5$. a–c) $A = 2$, $B = 0.5$, $\epsilon = 0$; d–e) $A = 1$, $B = 0.5$, $\epsilon = 0$, f–g) $A = 1$, $B = 0.5$, $\epsilon = 0.5$.

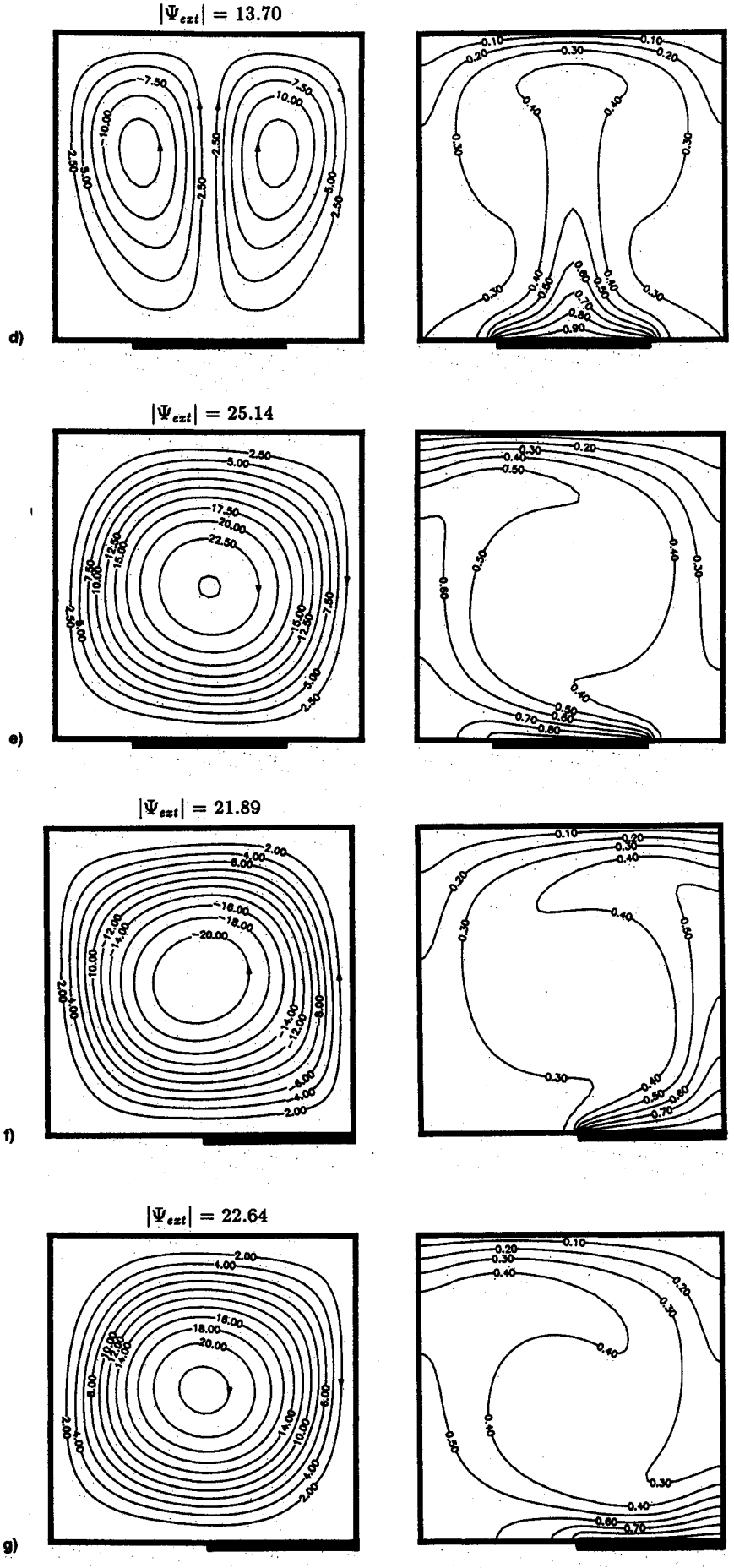

Fig. 2 Steady-state streamlines and isotherms for $Ra = 10^5$. a–c) $A = 2$, $B = 0.5$, $\epsilon = 0$; d–e) $A = 1$, $B = 0.5$, $\epsilon = 0$, f–g) $A = 1$, $B = 0.5$, $\epsilon = 0.5$.

second and this agreement with the results obtained from various authors as discussed by De Vahl Davis and Jones.[17] Finally it must be mentioned that, in the pure conduction regime ($Ra = 0$), the numerical model was found to predict the analytical solution, Eqs. (13) and (14), with an accuracy of 0.5%.

Results and Discussion

Flowfields, temperature fields, and heat transfer rates for ranges of Rayleigh numbers Ra, aspect ratio of the cavity A, size of the isothermal heat source B, and position of the heat source ϵ are examined in this section. All results are presented for $Pr = 0.72$.

Figures 2a–2g illustrate the various modes of convection that can be observed in a cavity for $Ra = 10^5$, $B = 0.5$, and some typical values of A and ϵ. Streamlines are shown on the left and isotherms on the right. The heat source on the bottom is indicated by a heavy line. As noted earlier, the solid walls have the value $\Psi = 0$. Positive and negative Ψ values correspond respectively to clockwise and counterclockwise circulation. Contour locations were determined by linear interpolation.

Figure 2a illustrates the flow and temperature fields obtained for a cavity of aspect ratio $A = 2$ with a centrally located heated element ($\epsilon = 0$) of size $B = 0.5$. For a cavity fully heated from below $B = 1$, the flowfield would consist of one pair of counter rotating cells. The final direction of rotation of the cells is not imposed by the physics of the problem but rather induced by the round-off errors generated in the numerical computation. In contrast, when the cavity is partially heated from below $B < 1$ the fluid being ascendant above the heated element, the direction of the rotation of the cells seems to be imposed a priori (see Fig. 2a). These flows, which develop from rest $\Psi = T = 0$, can be referred to as "natural" flows as defined by Walch and Dulieu[9] in their study of natural convection within slightly inclined rectangular cavity heated from below. However, it is also possible to obtain, under certain conditions that are discussed later, another steady-state flow pattern where the fluid motion above the heated element moves down toward it. Such a reversed circulation, which may be called "antinatural," is illustrated in Fig. 2b. To obtain antinatural flows, the initial conditions must be chosen carefully. Thus, the flow pattern in Fig. 2b was obtained in the following way: A pair of counter-rotating cells with a reversed circulation toward the heated element was

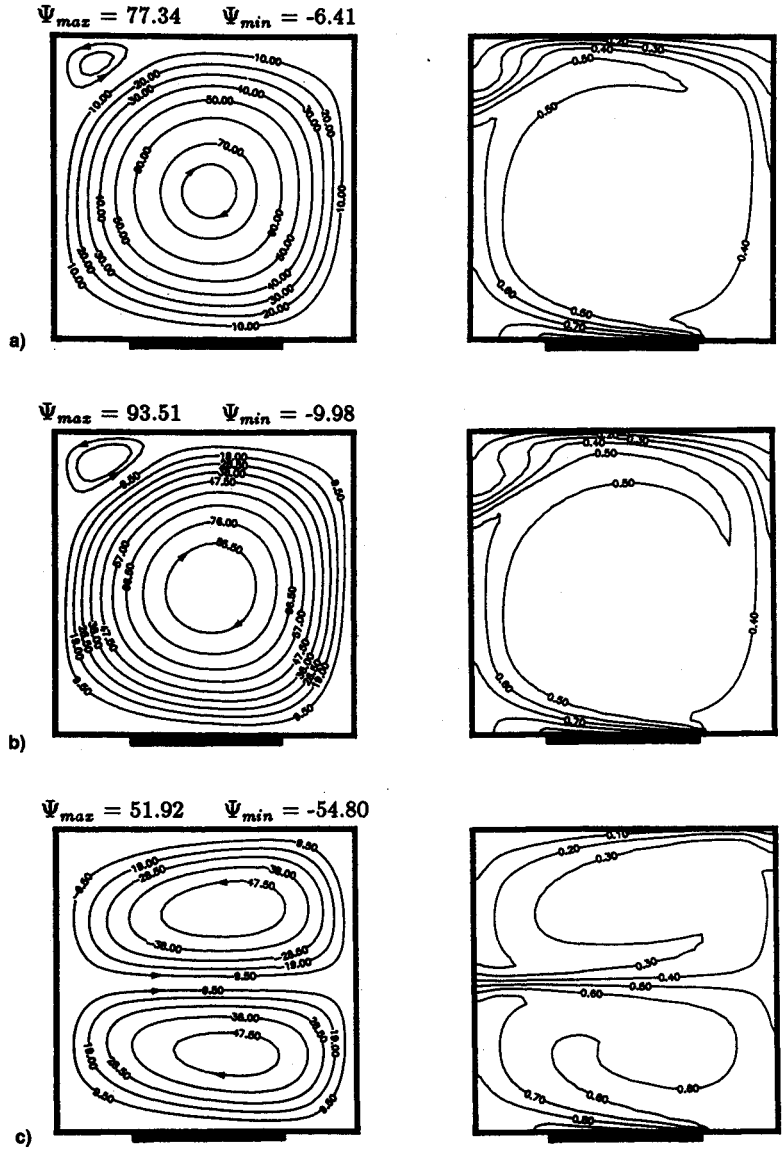

Fig. 3 Steady-state streamlines and isotherms showing the evolution of the unicellular convective mode with Ra. a) $Ra = 10^6$, b) $Ra = 1.5 \times 10^6$, c) $Ra = 2 \times 10^6$.

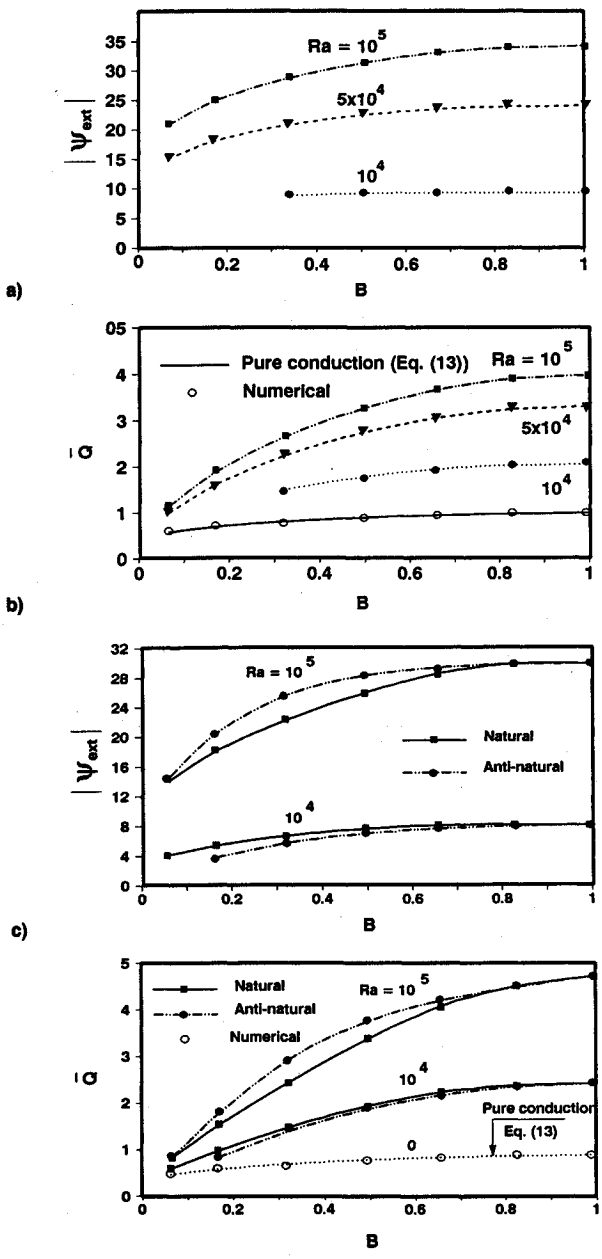

Fig. 4 Extremum stream function $|\Psi_{ext}|$ and average heat transfer $\bar{Q}$ as a function of size B for $A = 2$, and $\epsilon = 0$. a) and b) unicellular convective mode, $Ra = 10^4$, 5×10^4, and 10^5; c) and d) bicellular convective mode, $Ra = 10^4$ and 10^5.

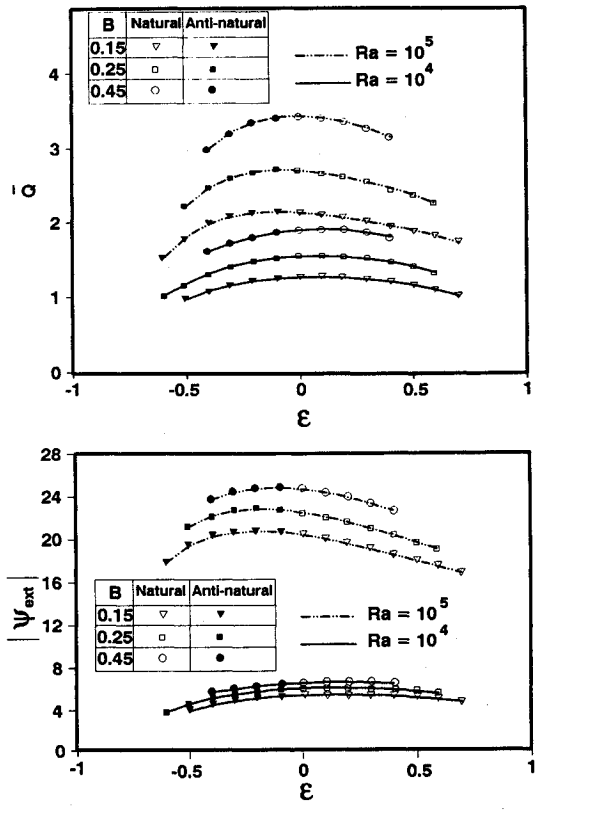

Fig. 5 a) Extremum stream function Ψ_{ext} and b) average heat transfer $\bar{Q}$ as a function of size B and eccentricity of heated element for $Ra = 10^5$ and 10^4.

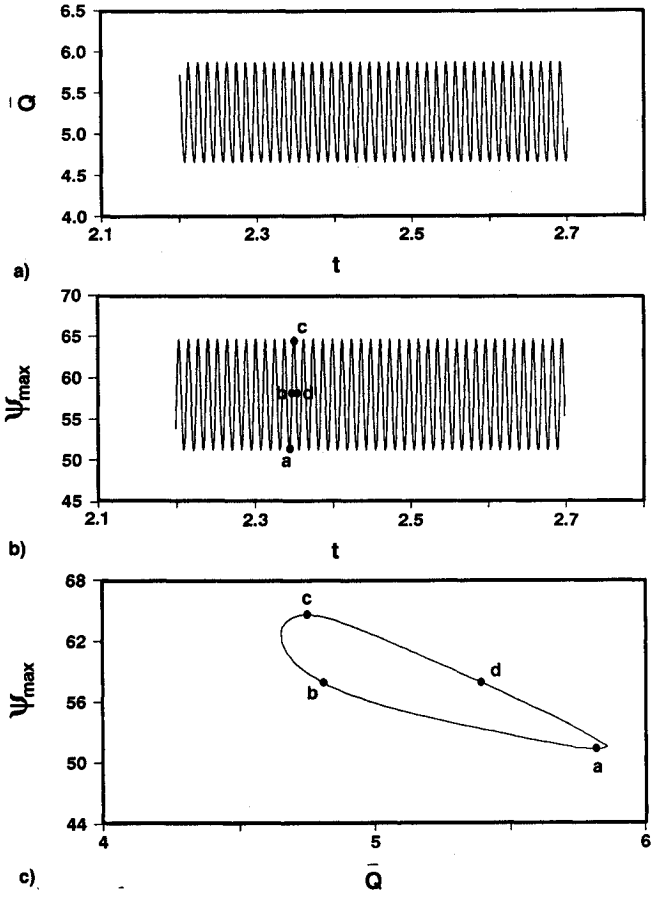

Fig. 6 Periodic solution for $Ra = 2.45 \times 10^6$, $A = 1$, $B = 0.5$, $\epsilon = 0.5$. a) Average heat transfer $\bar{Q}$ variation with t; b) maximum stream function Ψ_{max} variation with t; c) the trajectory in (Ψ_{max}, $\bar{Q}$) phase plane.

chosen as the initial condition of the evolutive problem. The initial "stirred" flow condition can be specified, for instance by Eq. (15), which allows initiation of m counter-rotating cells in the x direction. The isotherms in Figs. 2a and 2b show that in both natural and antinatural flows, the ascending streams are warmer than the descending ones, providing the driving force in the respective directions of motion. In general, for a given set of governing parameters, not only the two bicellular flow patterns discussed above can exist but other solutions with different number of cells are possible. For instance, Fig. 2c shows the steady-state solution associated with unicellular convection. The governing parameters are the same as those considered in Figs. 2a and 2b; but the initial conditions are different. Naturally, because the heated element in Fig. 2c is centrally located ($\epsilon = 0$), the unicellular convective cell can rotate indifferently in either direction as in a classical Bénard situation.

Figures 2d and 2e illustrate two possible convection modes for $A = 1$, $B = 0.5$, and $\epsilon = 0$. The antinatural solution that consists of two cells moving down toward the heated element

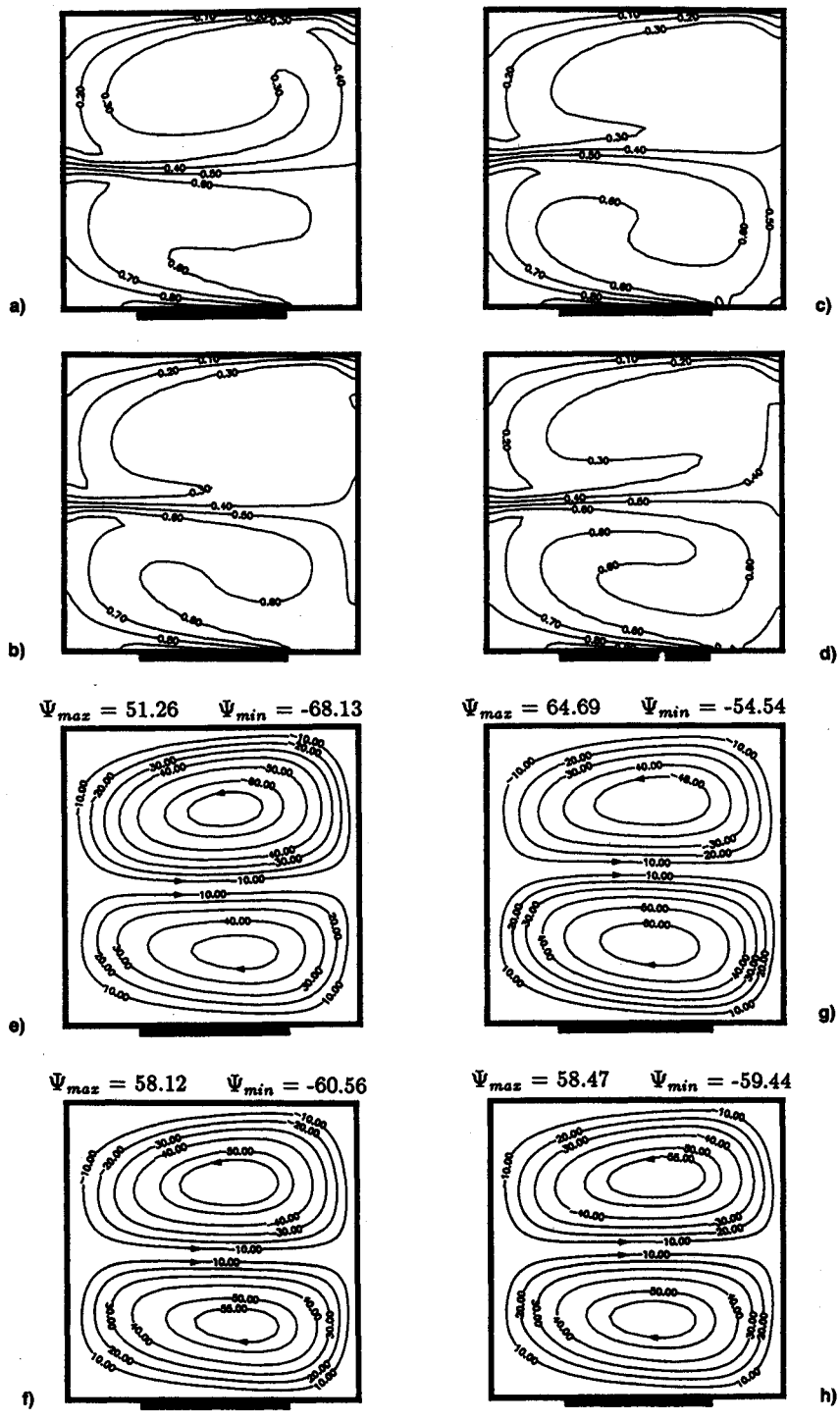

Fig. 7 Streamlines and isotherms over one complete cycle for $Ra = 2.45 \times 10^6$.

was impossible to reach despite the adequate choice of initial conditions. Generally, the final steady state achieved consists of one unicellular mode when the initial conditions are different from the rest.

Figures 2f and 2g show the steady-state solution obtained for a square cavity $A = 1$ when the heated element is moved to the right lower corner of the cavity $\epsilon = 0.5$. Using the rest state as initial values, the resulting flow pattern is similar to that of Fig. 2a except that the symmetry is now destroyed due to eccentricity of the heated element. As illustrated in Figs. 2f and 2g it is also possible, by using proper initial conditions, to sustain a unicellular circulation within the cavity. Although the unicellular counterclockwise circulation of Fig. 2f cannot be started from rest conditions, it will be referred in the present study as a "natural" flow because it corresponds to a situation where the fluid is ascending over the heated element. For the same reason, the clockwise circulation of Fig. 2g corresponds to an antinatural flow.

Figures 3a–3c show the evolution of the unicellular convective mode for $A = 1$, $B = 0.5$, $\epsilon = 0$, and Ra increasing up to 2×10^6. All these figures represent steady states. Hence, for moderate Rayleigh number $Ra = 10^5$, Fig. 2e shows small distortion of isotherms in the middle of the cavity. This distortion is amplified with increasing Ra producing a small negative cell in the left upper corner of the cavity in Fig. 3a for $Ra = 10^6$. Figure 3b shows another steady-state flow with more distortion at $Ra = 1.5 \times 10^6$ producing a more important negative cell with a stronger flow strength. At $Ra = 2$

$\times 10^6$, Fig. 3c shows that the distortion breaks down and the negative cell becomes as important as the positive cell.

Figures 4a and 4b show, respectively, the influence of B on $|\Psi_{ext}|$ and $\bar{Q}$ for $A = 2$, $\epsilon = 0$ and typical values of Rayleigh number. These graphs are derived for a unicellular flow where the fluid circulation within the cavity is indifferently clockwise or counterclockwise because the heated element is centrally located ($\epsilon = 0$). As it can be seen, for a given value of Rayleigh number, the flow strength and the heat transfer are increasing functions of B with a maximum values for a cavity fully heated from below. For $B > 0.6$, $\bar{Q}$ and $|\Psi_{ext}|$ variations are moderate. They become more pronounced for $B \leq 0.6$ and high Rayleigh numbers. For $Ra = 10^4$, $|\Psi_{ext}|$ variation is almost independent of B as far as the unicellular convection mode remains possible. Also, the heat transfer variation with B is weak. The reason for this is that the flow regime is not too far from the pure conduction regime at $Ra = 10^4$. Also, it is seen that there exists a critical value of B at about $B = 0.3$ for which the unicellular flow remains unstable. Hence, despite the adequate initializations to obtain a unicellular flow, the final steady-state solution is a bicellular one because the fluid circulation is poor and the energy given to the system is not enough to maintain the unicellular flow.

Figures 4c and 4d show, respectively, $|\Psi_{ext}|$ and Q vs B for $A = 2$, $\epsilon = 0$, and two values of Rayleigh number. To obtain a bicellular flow, the initial conditions were carefully chosen. In these graphs, it is seen that the antinatural solution gives better heat transfer and better flow circulation at $Ra = 10^5$ and B between 0.1 and 0.7. Similar observations were made in the past by Sen et al.[18] At $Ra = 10^4$, $|\Psi_{ext}|$ and $\bar{Q}$ are higher for the natural solution. Also, it can be observed that there is a critical value of B under which only the natural solution is possible independent of the initial conditions chosen.

The eccentricity effects on $|\Psi_{ext}|$ and $\bar{Q}$ are shown in Figs. 5a and 5b for $Ra = 10^5$ and 10^4 and $B = 0.15$, 0.25, and 0.45. The natural solutions are indicated by empty symbols and the antinatural solutions are indicated by filled symbols. All these results concern a unicellular flow. If the heated element is centrally located ($\epsilon = 0$), the solution is natural because the fluid circulation within the cavity may be indifferently clockwise or counterclockwise. For a positive eccentricity of the heated element $\epsilon > 0$, the natural flow is counterclockwise whereas for a negative eccentricity $\epsilon < 0$, it is clockwise. For a given B and Rayleigh number, Fig. 5b shows that the heat transfer increases first with increasing ϵ and it reaches a maximum and decreases after that. The locations of the maximums are dependent of B and Ra. For example, if $B = 0.25$, the maximum occurs at about $\epsilon \approx -0.11$ for $Ra = 10^5$ and at about $\epsilon \approx 0$ for $Ra = 10^4$. Similar trends can be observed on Fig. 5a for $|\Psi_{ext}|$ variations.

In order to prove the existence of the oscillatory behavior of the flow and heat transfer at high Rayleigh numbers, the values of the parameters A, B, and ϵ were arbitrarily fixed to 1.0, 0.5, and 0.0, respectively. Because two solutions are possible for these specified parameters at a given moderate Rayleigh number as demonstrated before, two ways can be followed to reach the convective oscillatory mode.

The first is to initialize the problem from a unicellular convective mode. The steady-state flow remains possible until $Ra = 2.4 \times 10^6$. For $Ra = 2.45 \times 10^6$, a sustained oscillatory convection is obtained, as shown in Figs. 6a and 6b. To ensure that the nature of oscillation is sustained, the time integration was continued up to $t = 6$ for all the oscillatory solutions. The stable oscillations depicted in Figs. 6a and 6b are sinusoidal and characterized by the same oscillation period. As a result, the projection on the $(\Psi_{max}, \bar{Q})$ plane gives a single

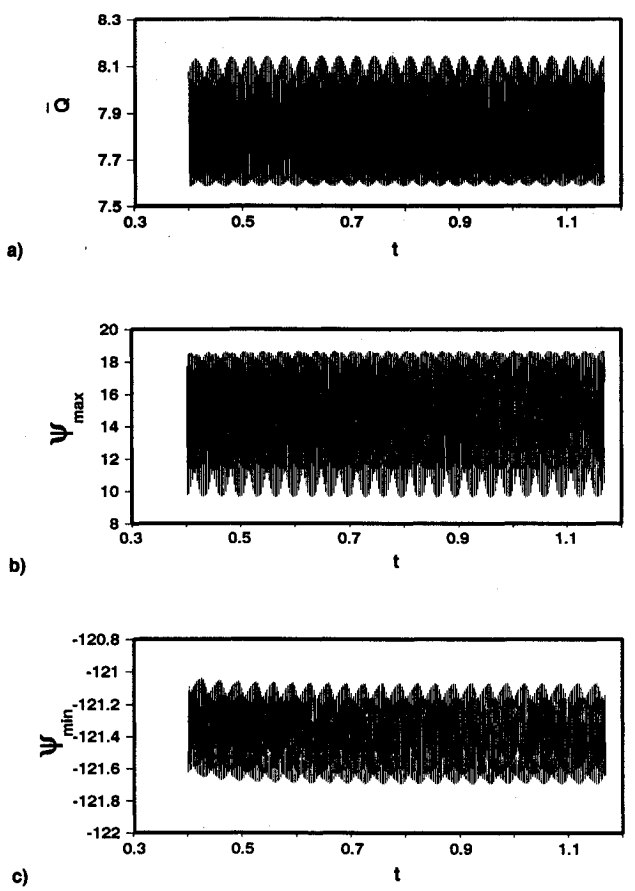

Fig. 8 Periodic solution for $Ra = 2.45 \times 10^6$, $A = 1$, $B = 0.5$, and $\epsilon = 0.5$. a) Average heat transfer $\bar{Q}$ variation with t; b) maximum stream function Ψ_{max} variation with t; c) minimum stream function Ψ_{min} variation with t.

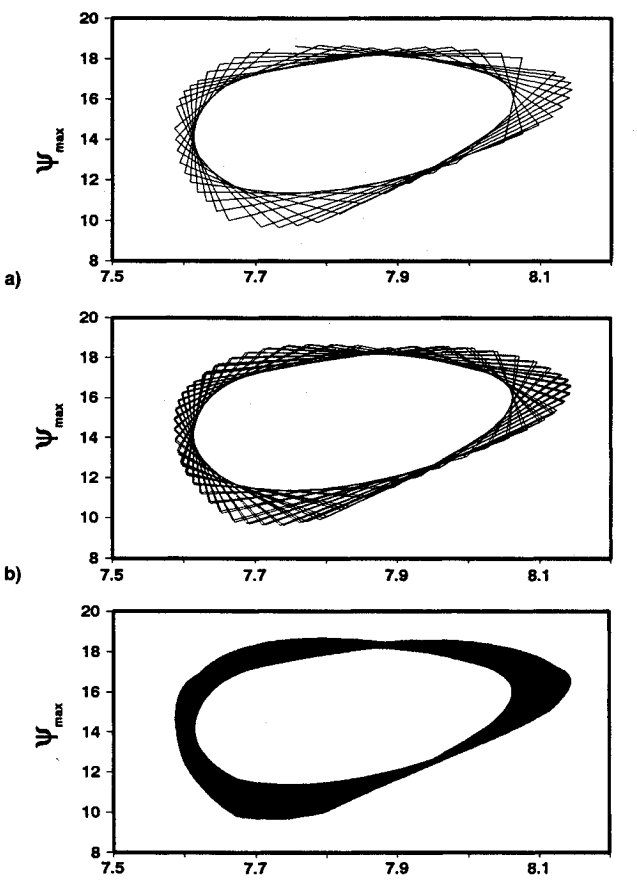

Fig. 9 The trajectory in $(\Psi_{max}, \bar{Q})$ phase plane for $Ra = 2.45 \times 10^6$, $A = 1$, $B = 0.5$ and $\epsilon = 0$. a) Relatively short period of time; b) about double the period of time in part a; c) long period of time.

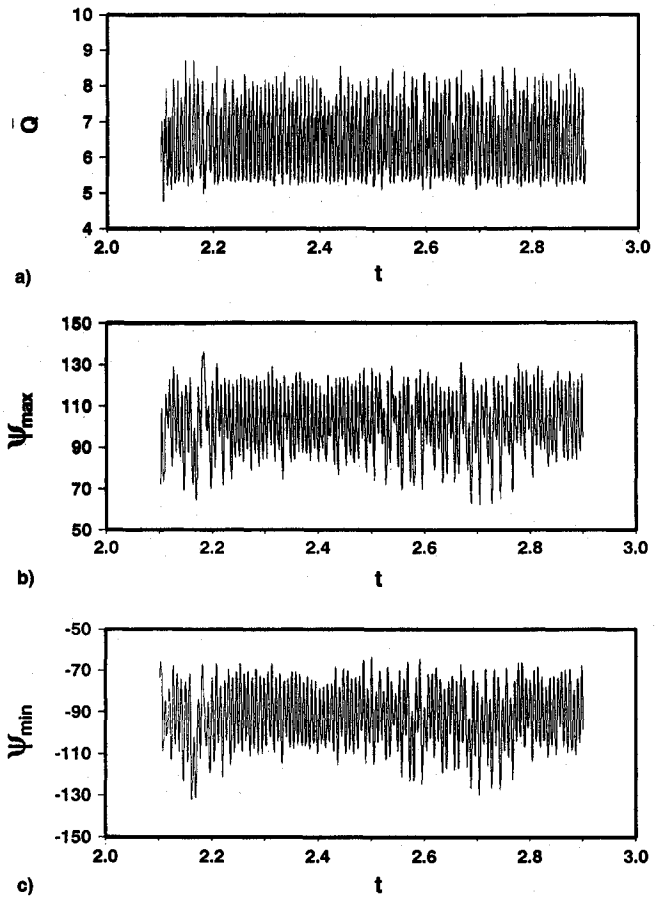

Fig. 10 Chaotic behavior for $Ra = 5 \times 10^6$, $A = 1$, $B = 0.5$, and $\epsilon = 0$. a) Average heat transfer $\bar{Q}$ variation with t; b) maximum stream function Ψ_{max} variation with t; c) minimum stream function Ψ_{min} variation with t.

closed curve as presented in Fig. 6c. According to the convention of Lennie et al.,[19] the oscillatory patterns are denoted as P_1, P_2, . . ., P_n, etc., depending on the number of cycles n per period. Hence, Fig. 6c gives a P_1 solution. Figs. 7a–7d show streamlines and isotherms for $Ra = 2.45 \times 10^6$ and at the time-steps indicated with a, b, c, and d in Fig. 6b, during a single oscillation of the flow. As it can be seen in Figs. 7a–7d, the form of the streamlines does not vary much. It can also be seen that Ψ_{max} takes importance to the detriment of Ψ_{min} between a to b to c and loses importance in consideration of Ψ_{min} between a to b to c. The corresponding isotherms are consequently affected.

The second method is to initialize the problem from a bicellular convective mode. In this case, the two cells remain stable until $Ra = 8 \times 10^5$. For $Ra = 10^6$, the steady-state solution is the same as in Fig. 3a, despite the initialization with a bicellular convective mode. As indicated before, this solution was an outcome of a unicellular initialization. The oscillatory convective mode is different for the second kind of initialization as seen in Figs. 8a–8c for $Ra = 2.45 \times 10^6$, $A = 1$, $B = 0.5$, and $\epsilon = 0$. The nature of the oscillations is also periodic but much more complicated. The period of the oscillations is the same for $\bar{Q}$, Ψ_{max}, and Ψ_{min}. During each time-step, the variation of Ψ_{max} (Ψ_{min} (not shown here)) vs $\bar{Q}$ is a segment tangent to an ellipse in (Ψ_{max}, $\bar{Q}$) plane as shown in Fig. 9a. Figure 9b shows the evolution of Ψ_{max} vs $\bar{Q}$ in the same plane for a relatively long time period than in Fig. 9a. All the space between the ellipse and its envelope has been swept by the segments when the period time considered was long enough (Fig. 9c). This kind of convection oscillatory mode is qualitatively different from that described in Figs. 6a–6c. Only the Ψ_{max} amplitude oscillation is important while Ψ_{min} amplitude oscillation is very weak as depicted in Figs. 8b–8c. By increasing Ra up to 5×10^6, the periodic oscillations give way to a chaotic one as seen in Figs. 10a–10c. The fluctuations are seen to be much larger in magnitude in comparison with the periodic oscillations obtained in Figs. 6a–6c for the same initial conditions; this indicates a vigorous convection.

Conclusions

A two-dimensional numerical study of natural convection heat transfer in an enclosed cavity with localized heating from below has been carried out. Multiple steady-state solutions, as well as periodic and nonperiodic solutions have been obtained by solving the Navier-Stokes and energy equations, utilizing the Boussinesq approximation. The following conclusions can be made:

1) The existence of a multiplicity of steady-state solutions for the present problem has been demonstrated numerically through the use of appropriate initial perturbations. Single- and multiple-cell convection take place, depending on the aspect ratio, Rayleigh number, dimensionless length of the heated segment, and its eccentricity. When two cells are involved, the solution is termed natural or antinatural, depending on whether the fluid motion above the heated element is upward or downward. The natural solution may be obtained for any values of the governing parameters (Ra, A, B, ϵ) investigated, because there are always driving forces from the pure conduction temperature field acting to initiate that flow. The antinatural solution requires a Rayleigh number above a critical value that is a function of the parameters A, B, and ϵ, and the number of cells within the cavity.

2) For a given set of the governing parameters, as the Rayleigh number is above a critical value, periodic and nonperiodic solutions are observed. The existence of two different periodic oscillatory behaviors for the same governing parameters is demonstrated with each periodic oscillatory behavior dependent on the initial conditions. For $A = 1$, $B = 0.5$, and $\epsilon = 0$, the unicellular mode remains $Ra = 8 \times 10^5$. A small negative cell appears in the left upper corner of the cavity at $Ra = 1 \times 10^6$. The negative cell becomes as important as the positive one with two cells, one on top of the other, at $Ra = 2 \times 10^6$.

3) Past studies have considered the present problem for the particular case where the heated element is centrally located $\epsilon = 0$. Owing to the symmetry of the problem, only half of the cavity was considered for computational purposes in order to "save computational time." However, as demonstrated by the present study, a host of nonsymmetric solutions may exist in a problem possessing "symmetry" in its geometry and boundary conditions. Thus, the use of the symmetry in numerical simulations of similar problems should be done cautiously.

The multiplicity of solutions involved in this work closely parallels those of natural convection in a closed circulation loop (Acosta et al.[13]) and in slightly inclined cavity with opposite walls at different temperatures (Moya et al.,[11] Walch and Dulieu[9]).

Acknowledgment

This work was supported in part by the Natural Sciences and Engineering Research Council of Canada and jointly by the FCAR Government of Quebec.

References

[1]Ostrach, S., "Natural Convection in Enclosures," *Advances in Heat Transfer*, Vol. 8, 1972, pp. 161–227.

[2]Catton, I., "Natural Convection in Enclosures," *Proceedings of the Sixth International Heat Transfer Conference*, Vol. 6, 1978, pp. 13–31.

[3]Torrance, K. E., and Rockett, J. A., "Numerical Study of Natural Convection in an Enclosure with Localized Heating From Below—Creeping Flow to the Onset of Laminar Instability," *Journal of Fluid*

Mechanics, Vol. 36, 1969, pp. 33–54.

[4]Torrance, K. E., Orloff, L., and Rockett, J. A., "Experiments on Natural Convection in Enclosures with Localized Heating from Below," *Journal of Fluid Mechanics*, Vol. 36, 1969, pp. 21–31.

[5]Tamotsu, H., Utaro, I., and Teiriki, T., "Heat Transfer by Natural Convection in an Enclosed Cavity—A Part of Bottom is Heated," Kagaku Kogaku Ronbunshu, Vol. 1, 1975, pp. 450–453 (in Japanese).

[6]Chao, P., Ozoe, H., Churchill, S., and Lior, N., "Laminar Natural Convection in an Inclined Rectangular Box with the Lower Surface Half-Heated and Half-Insulated," *Journal of Heat Transfer*, Vol. 105, 1983, pp. 425–432.

[7]Kamotani, Y., Wang, L. W., and Ostrach, S., "Natural Convection Heat Transfer in a Water Layer with Localized Heating from Below," *The Twenty-first National Heat Transfer Conference*, Seattle, WA, HTD, Vol. 26, 1983, pp. 43–48.

[8]Fuseki, T., and Farouk, B., "Natural Convection in a Thermally Stratified Square Cavity with Localized Heating from Below," *National Heat Transfer Conference*, Denver, CO, Paper 85-HT-34, 1985.

[9]Walch, J. P., and Dulieu, B., "Convection de Raleigh-Bénard dans une cavité poreuse faiblement inclinée," *Journal de Physique. Lettres*, Vol. 43, 1982, pp. L103–L107.

[10]Caltagirone, J. P., and Bories, B., "Solution and Stability Criteria of Natural Convective Flow in an Inclined Porous Layer," *Journal of Fluid Mechanics*, Vol. 30, 1985, pp. 741–756.

[11]Moya, S. L., Ramos, F., and Sen, M., "Numerical Study of Natural Convection in a Tilted Rectangular Porous Material," *International Journal of Heat and Mass Transfer*, Vol. 30, 1987, pp. 741–756.

[12]Robillard, L., Wang, C. H., and Vasseur, P., "Multiple Steady States in a Confined Porous Medium with Localized Heating from Below," *Numerical Heat Transfer*, Vol. 13, 1988, pp. 91–110.

[13]Acosta, R., Sen, M., and Ramos, E., "Single-Phase Natural Circulation in a Tilted Square Loop," *Waerme-und Stoffuebertragung*, Vol. 21, 1987, pp. 269–275.

[14]Hahne, E., and Schallig, R., "Formfaktoren der Waermeleitung fur Anordnungen mit Isothermen Rippen," *Waerme-und Stoffuebertragung*, Vol. 5, 1972, pp. 39–46.

[15]Ozoe, H., and Sayama, H., "Natural Convection in an Inclined Square Channel," *International Journal of Heat and Mass Transfer*, Vol. 17, 1974, pp. 401–406.

[16]De Vahl Davis, G., "Natural Convection of Air in a Square Cavity: A Bench Mark Numerical Solution," *International Journal for Numerical Methods in Fluids*, Vol. 3, 1983, pp. 249–264.

[17]De Vahl Davis, G., and Jones, I. P., 1983, "Natural Convection in a Square Cavity: A Comparison Exercise,"*International Journal for Numerical Methods in Fluids*, Vol. 3, pp. 227–248.

[18]Şen, M., Vasseur, P., and Robillard, L., "Multiple Steady States for Unicellular Natural Convection in an Inclined Porous Layer," *Journal of Heat and Mass Transfer*, Vol. 30, No. 10, 1987, pp. 2097–2113.

[19]Lennie, T. B., McKenzie, D. P., Moore, D. R., and Weiss, N. O., "The Breakdown of Steady Convection,"*Journal of Fluid Mechanics*, Vol. 188, 1988, pp. 47–85.

Recommended Reading from the AIAA Progress in Astronautics and Aeronautics Series . . . AIAA

Spacecraft Dielectric Material Properties and Spacecraft Charging

Arthur R. Frederickson, David B. Cotts, James A. Wall and Frank L. Bouquet, editors

This book treats a confluence of the disciplines of spacecraft charging, polymer chemistry, and radiation effects to help satellite designers choose dielectrics, especially polymers, that avoid charging problems. It proposes promising conductive polymer candidates, and indicates by example and by reference to the literature how the conductivity and radiation hardness of dielectrics in general can be tested. The field of semi-insulating polymers is beginning to blossom and provides most of the current information. The book surveys a great deal of literature on existing and potential polymers proposed for noncharging spacecraft applications. Some of the difficulties of accelerated testing are discussed, and suggestions for their resolution are made. The discussion includes extensive reference to the literature on conductivity measurements.

***TO ORDER:* Write, Phone, or FAX:** American Institute of Aeronautics and Astronautics c/o Publications Customer Service, 9 Jay Gould Ct., P.O. Box 753, Waldorf, MD 20604 Phone: 301/645-5643 or 1-800/682-AIAA, Dept. 415 ■ FAX: 301/843-0159

Sales Tax: CA residents, 8.25%; DC, 6%. For shipping and handling add $4.75 for 1–4 books (call for rates for higher quanties). Orders under $50.00 must be prepaid. Foreign orders must be prepaid. Please allow 4 weeks for delivery. Prices are subject to change without notice. Returns will be accepted within 15 days.

1986 96 pp., illus. Hardback
ISBN 0-930403-17-7
AIAA Members $29.95
Nonmembers $37.95
Order Number V-107